Int. J. of Applied Mechanics and Engineering, 2022, vol.27, No.2, pp.143-157
DOI: 10.2478/ijame-2022-0025

PROMISING WING VIBRATION MEASUREMENT SYSTEM USING MEMS IMUS AND KALMAN FILTER CORRECTION

M.S. MAAMO[*1], A.A. AFONIN[1,2] and A.S. SULAKOV[1]
[1]Moscow Aviation Institute (National Research University), Moscow, RUSSIAN FEDERATION
[2]Moscow University for Industry and Finance «Synergy» Moscow, RUSSIAN FEDERATION
E-mail: mhd.maamo@gmail.com

Nowadays, there is still a need for the development of a high-precision vibration measurement system for aircraft wings. By analyzing the wing vibration characteristics a lot of aviation studies could be conducted, including the wing health monitoring, the fluttering phenomenon and so on. This paper presents preliminary results of the research carried out toward building a promising system designed to measure vibration parameters of aircraft wing. Comparing it with the existing analogue systems, the proposed system features the use of approaches that are traditional for solving orientation and navigation problems for vibration measurements. The paper presents the basic structure of the system, the fundamentals of its operation, the mathematical errors models of its main components, the correction algorithms using optimal Kalman filter. Finally, the initial simulation results of system operation are shown, demonstrating the expected accuracy characteristics of the system, which confirms its effectiveness and the prospects of the chosen direction of research.

Keywords: aircraft wing, vibration measurement, Kalman filter, MEMS IMU, closed-loop optimal correction.

1. Introduction

Nowadays, due to the ever-increasing degree of complexity of aircraft design, production and operation, the improvement of existing methods and the development of new ones for measuring vibration parameters of aircraft mechanical structures, in particular, aircraft wing, is considered as an important field of research and development. On the basis of vibration measurements a wide range of aviation problems is solved, including: vibration diagnostics, passive and active vibration isolation, modal analysis, and so on [1-4]. Besides, it is noteworthy that the use of structures made of thin-walled beams as the main structural components in modern aircrafts has currently expanded significantly, which is practically associated with the emergence and spread of fibrous composite materials. For example, there are new produced wings that provide a high strength-to-weight ratio, better corrosion resistance and better fatigue life in comparison to the wings produced from traditional materials. However, this comes with a cost, that is, such aircrafts tend to be very flexible, demonstrating, for example, large wing deformations under normal operating loads, which significantly affect their aerodynamic and strength characteristics. Therefore, the use of vibration parameters measurement system (VPMS) of the wings becomes very necessary for wing health monitoring, even in-flight operation mode [5-8]. VPMS design largely depends on the choice of vibration sensors. To measure aircraft wing vibrations, the following types of sensors are often used: piezoelectric accelerometers, optical sensors and MEMS accelerometers [7-10]. The main advantages of VPMS, built on the basis of piezoelectric accelerometers, include: sufficient accuracy, resistance to vibrations, shock and high temperatures. Its disadvantages include: high cost and power consumption, significant weight and dimensions, taking into ac-count the mounting and auxiliary devices, which, for example, have especial negative effects during experimental studies of aircraft wing properties, since in this case it is necessary to use a large number of sensors with relatively bulky charge amplifiers. In addition, traditional mounting methods, beside the weight and dimensions of these sensors, negatively affect the

[*] To whom correspondence should be addressed

frequency range of measurements, causing distortion of the frequency properties of the objects under study (especially small-sized thin-walled ones), and make it difficult to use VPMS in the main operation modes of aircraft. Distortions of signals also occur when measuring low-frequency accelerations, leading to significant errors in integration to calculate vibration velocity and vibration displacement. VPMS, built on the basis of optical sensors, has the following advantages: sufficient accuracy; non-contact nature, i.e. there is practically no distortion of the true vibration shape of the objects under study; insensitivity to magnetic fields, electrostatic interference and ionizing radiation. The disadvantages of such VPMS include: significant weight, dimensions, power consumption, high cost, the possibility of false measurements when operating in conditions like high dustiness, fog, intense ambient light, low temperatures, strong vibrations, which would complicate its use during the in-flight mode. Moreover, the procedure for aligning the optical axes of the emitters and receivers of such sensors during installation is very laborious, and the signal processing algorithms of such VPMS require the use of very high-performance computers. VPMS, built on the basis of MEMS accelerometers, has the following advantages: small weight, dimensions, cost, and power consumption; slight distortion of signals in low frequency range; the possibility of using it for testing small-sized and thin-walled structures without significant distortion of the true vibration shape, especially that these accelerometers offer the possibility of wireless transmission of signal. The disadvantages of MEMS accelerometers include: relatively low accuracy and significant instability of their characteristics. On the other hand, due to the rapid development of micromechanical technology and the emergence of a new generation of sensors, in particular micromechanical inertial measurement units (MEMS IMUs), which include integrated three-components micromechanical gyroscopes and accelerometers, and sometimes other sensors like: magnetometer, temperature sensor, barometer and so on, a new development and research direction has been opened based on the integration of such MEMS sensors into measurement systems. The primary use of such MEMS IMU is to simultaneously measure the projections of both apparent acceleration and absolute angular velocity in the associated with the object coordinate system (ACS), and it has found a wide application in the field of navigation and motion control. On the other hand, these MEMS IMUs can give a complete information about the movement parameters of the measurement point of the mechanical structure under study. So, we suggest that on the basis of this information it is easy to find the vibration characteristics of the mechanical structure under test. Unlike piezoelectric accelerometer, even a cheap MEMS IMU operates without significant distortions at both high and low frequencies and is characterized by small mass-dimensions characteristics, which allow its use with small-sized structures without significant distortion of the true vibration shape of the object under study. Moreover, MEMS IMU can sometimes be included in the information processing system wirelessly, which, in particular, simplifies its installation. In addition, the new generation of MEMS IMU includes accelerometers and gyroscopes with frequency responses more than *300* Hz and *700* Hz, respectively [11], which is very adequate to measure wings vibrations [12, 13]. Nevertheless, MEMS IMUs are usually known for many disadvantages, mainly their low accuracy and significant instability of their characteristics. In this regard, a large number of research and development works are devoted to the issues of constructing errors models of MEMS IMU and researching ways to reduce them, as well as to improve its calibration procedures. In addition, to eliminate the indicated drawbacks of MEMS IMU, optimal Kalman estimation and correction algorithms, as well as the technology of sensor data fusion technics, have been widely used [14-18]. Thus, in our case, it is proposed to construct VPMS based on MEMS IMUs using the technology of sensor data fusion and optimal Kalman estimation. Consequently, the proposed VPMS will predominantly have common features with the VPMS based on MEMS accelerometers, as well as to some extent with the VPMS based on piezoelectric accelerometers, and at the same time it will be able to overcome their main disadvantages noted earlier. The key advantages of the proposed VPMS will be a sufficiently high accuracy, due to the use of complex optimal processing of data from different sources, including MEMS IMU, the aircraft onboard navigation system (NS), as well as the displacement sensor (DS) like strain gauge or fiber optic sensor [19], which will make it possible to evaluate and correct the basic errors of the system as a whole. In addition, the system would provide other benefits such as low cost and power consumption, small weight and dimensions, as well as the simplicity of equipping the aircraft with a system of this type, thanks to the relatively simple installation of MEMS IMU at the measurement point. Besides, the system is supposed to be able to work both in a stationary state of the object (in laboratory and factory conditions), and during the operation of the object (including aerodrome or in-flight operations). In this regard, it should be mentioned that most modern aircrafts have their own NS, and some promising aircrafts are equipped with DS embedded into their main structural elements, for example, in the wings. In order to obtain the previously mentioned advantages of the proposed system, the algorithms that determine the orientation and navigation parameters based on low-accuracy MEMS IMU data should use correction signals from other measurement transducers, in this case the DS and aircraft NS (see Fig.1). Besides, incorporation of optimal Kalman filter (OKF) based on open-loop scheme [20] gives acceptable results only for a limited period of time [21], after which a significant increase in estimation errors for a number of parameters arises. This is due to many reasons, including the limited accuracy of the MEMS IMU error models and the orientation and navigation channels which work based on them, as well as the DS, which becomes apparent especially sharply with their large intrinsic errors arising from long-term operation. To solve this problem, it is advised to apply the closed-loop correction technique of movement parameters [22]. In this case appropriate correction signals are fed back at certain points of the system in order to prevent the growth of intrinsic errors of MEMS IMUs and DS, and consequently of the orientation and navigation channels, and keep them at the levels that OKF optimal estimation can afford. The correction signal is formed as a product of the measurement vector by Kalman filter optimal gains matrix $\boldsymbol{K}$ (8.1). This method of generating correction signals significantly reduces the required amount of calculations, because in this case there is no need to calculate error estimates. So, in this work, rational approaches and methods of research and development of the proposed VPMS are selected, built on the basis of fusion and processing the data of MEMS IMUs, DS and onboard NS using OKF. A variant of the proposed system structure and components for the case of measuring the aircraft wing vibrations is proposed and analyzed. The errors models of system components are developed. The main operation algorithms are developed, including an optimal estimation algorithm of the errors and their corrections, as well as an algorithm for calculating the main vibration parameters, including vibration displacement, vibration velocity and vibration acceleration. At the end of this paper, the results of system simulation are presented, confirming the functionality and perspectivity of the proposed VPMS in view of its capability to achieve acceptable accuracy characteristics for vibration parameters measurement.

2. Methods and materials

The purpose of this work is to analyze the possibility and prospects of constructing a system for measuring the vibrations of an aircraft wing, based on the use of MEMS IMU as its main vibrometer. In this case, the object of research is the vibration parameters measurement system, and the subject is its structure, components, operation algorithms and expected accuracy characteristics. To achieve this goal, an information-measurement system is built essentially on the basis of inertial devices, beside the use of sensors for indirect measurement of displacement. In this context, numerical and analytical methods of higher mathematics and theoretical mechanics, methods of the theory of random processes and optimal estimation are used [18, 21, 24]. The MathCAD environment is used to carry out a simulation of system operation. The purpose of modeling the operation of VPMS with permissible characteristics in conditions close to reality is to assess the final expected accuracy of measuring the vibration parameters.

3. Wing vibration measurement system-basic structure

A basic structure and hardware components scheme of VPMS is shown in Fig.1, where $\boldsymbol{R}_N$ is geocentric radius vector of point O , measured by the NS; $\boldsymbol{R}_{M\,1}$ is the geocentric radius vector of point O_1 position, measured based on MEMS IMU1 readings; $\boldsymbol{R}_{M\,2}$ is the geocentric radius vector of point O_2, measured based on MEMS IMU2 readings; $\boldsymbol{R}_{K\,1}$ is the vector characterizing the position of O_1 relative to O; $\boldsymbol{R}_{K\,2}$ is the vector characterizing the position of O_2 relative to O_1, measured by DS; $\boldsymbol{u}$ is the vector of the angular velocity of Earth's own rotation; XYZ is the right coordinate system associated with each MEMS IMU and the NS (ACS), where the $\boldsymbol{X}$ axis is directed along its longitudinal axis, and the $\boldsymbol{Z}$ axis directed along the right wing. For VPMS, the right Earth equatorial (Greenwich) coordinate system (ECS) was chosen as a measurement base coordinate system, with the origin in the center of the Earth (O_E), whereas the unit vectors are $\xi,\eta,\zeta,$ where ξ lies at the intersection of the equator and Greenwich meridian planes, ζ is directed along the axis of rotation of the Earth. As it could be seen from Fig.1, in order to measure the vibrations of aircraft wing, one MEMS IMU unit is installed at its end (called here MEMS IMU2), and a DS is cemented along the wing, and another MEMS IMU unit (called here MEMS IMU1) is installed on the base (the fuselage for example) close to the start of the wing. In this case, VPMS contains two MEMS IMU units and DS, in addition to the onboard NS as an additional source of information. In this way, the suggested VPMS implements data fusion techniques based on the information provided by all these sensors (as sources of information). By applying the optimal Kalman estimations, the system can accurately measure the wing vibration parameters. It is worth mentioning that, when using the proposed VPMS in flight mode, it is advisable to make use of the information offered by the onboard NS (as illustrated in Fig.1), whereas other sources of information about the wing coordinates can be used when conducting ground tests. This structure gives the proposed VPMS another important advantage, that is its flexibility in introducing additional points when it is intended to measure the vibrations of much more complex structures, as in the case of an aircraft wing with a variable sweep. To do this, an additional MEMS IMU unit needs to be installed at each of the new measurement points, beside its own DS. Notice also that, traditional NSs form their output parameters vectors with a limited frequency. Consequently, the direct use of NS for adequate measurement of aircraft vibration parameters is possible, and even preferrable because of its high accuracy, only in a limited frequency range (up to 10 Hz). In such cases, MEMS IMU1 can be excluded, and the NS is directly used instead.

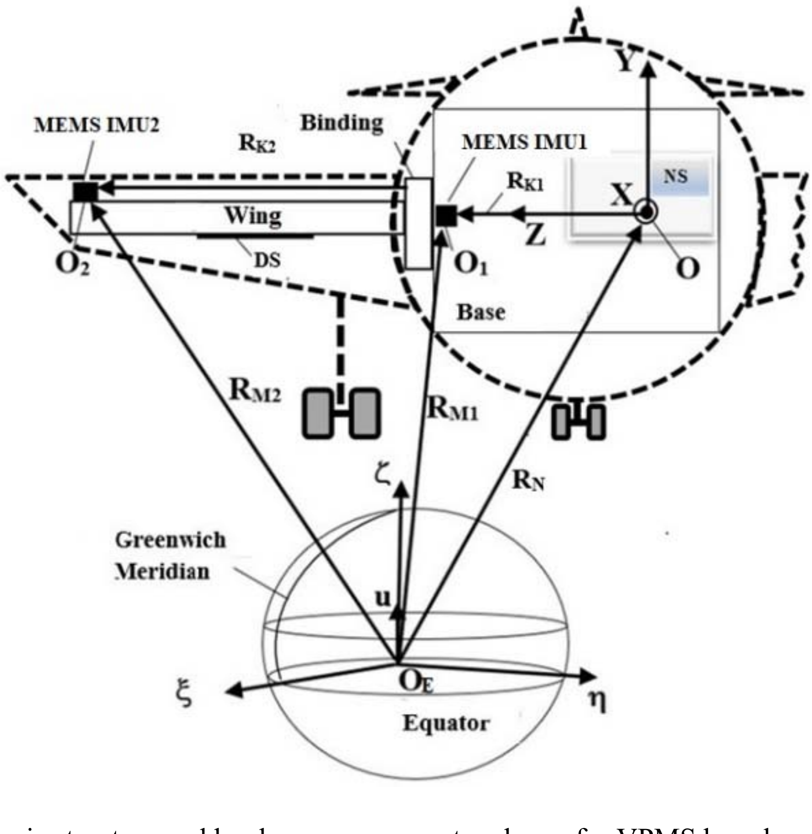

Fig.1. A variant of basic structure and hardware components scheme for VPMS based on MEMS IMUs.

4. Basic inertial navigation algorithm

The algorithm of determining orientation and navigation parameters is implemented in ECS. The corresponding equations have the following form in vector-matrix representation [23]:

$$\dot{\Lambda} = 0,5 M_{\omega_o} \Lambda,$$

$$A_{O/E} = \begin{pmatrix} \cos(u_0 t) & \sin(u_0 t) & 0 \\ -\sin(u_0 t) & \cos(u_0 t) & 0 \\ 0 & 0 & 1 \end{pmatrix} \left[\left(2\lambda_0^2 - 1 \right) E + 2\lambda\lambda^{\mathrm{T}} - 2\lambda_0 K_\lambda \right], \tag{4.1}$$

$$\dot{U} = -2u \times U + A_{O/E} n_O + g_N,$$

$$\dot{R} = U$$

where the index O indicates that the corresponding vector is presented by its projections on the ACS axes, whereas without the index means it is presented on the ECS axes; $A_{O/E}$ is the orientation matrix of ECS relative to ACS; R is the geocentric radius-vector of the measurement point (to which MEMS IMU is bonded); U is its relative velocity vector; $\dot{U}$ is its relative acceleration vector; n_O, ω_O are apparent acceleration vector and absolute angular velocity vector of MEMS IMU (or measurement point) as projections on ACS axes, measured by the accelerometers unit (AU) and gyroscopes unit (GU), respectively; $\lambda_0, \lambda_1, \lambda_2, \lambda_3$ are Rodrigues-Hamilton parameters [24], $\Lambda = [\lambda_0, \lambda_1, \lambda_2, \lambda_3]^{\mathrm{T}}$, $\lambda = [\lambda_1, \lambda_2, \lambda_3]^{\mathrm{T}}$; g_N is the vector of gravitational acceleration at the measurement point (to which MEMS IMU is bonded), it is normal to the Earth surface at the considered point; E is the unit matrix; t is time; u_0 is the module of u; K_λ is the skew-symmetric matrix composed of λ elements; M_{ω_O} is the skew-symmetric (quaternionic) 4x4 matrix composed of ω_O projections.

5. Mathematical errors model of the orientation and navigation parameters channel

The mathematical errors model of the orientation and navigation parameters channel used in the VPMS algorithm is obtained by applying the method of variation to the ideal operation algorithm [20]:

$$\dot{\theta} = -u \times \theta - A_{O/E}(\Delta\omega_{sys} + \Delta\omega_{wn} + \Delta\omega_{stoc} + \Delta\mathbf{k}_{s\omega}\omega_O),$$

$$\delta\dot{U} = -2u \times \delta U + A_{O/E}(\Delta n_{sys} + \Delta n_{wn} + \Delta n_{stoc} + \Delta\mathbf{k}_{sn} n_O) +$$
$$-\theta \times (A_{O/E} n_O) - \omega_0^2 \left(\delta R - 3 \left(\delta R \cdot 1_R \right) 1_R \right), \tag{5.1}$$

$$\delta\dot{R} = \delta U, \quad \Delta\dot{\omega}_{sys} = 0, \quad \Delta\dot{n}_{sys} = 0, \quad \Delta\dot{\omega}_{stoc} = -\mu_\omega \Delta\omega_{stoc} + \sigma_\omega \mathbf{u}_{f\omega},$$

$$\Delta\dot{n}_{stoc} = -\mu_n \Delta n_{stoc} + \sigma_n \mathbf{u}_{fn}, \quad \Delta\dot{\mathbf{k}}_{s\omega} = 0, \quad \Delta\dot{\mathbf{k}}_{sn} = 0$$

where δX represents the error of the corresponding quantity X; θ is the vector of small rotations characterizing the inclination of ECS calculated position relative to its true position; $\Delta\omega_{sys}$, Δn_{sys} are vectors of systematic errors components of AU and GU, respectively; $\Delta\omega_{wn}$, Δn_{wn} are vectors of their random components in the form of white noise; $\Delta\omega_{stoc}$, Δn_{stoc} are vectors of their random (stochastic) autocorrelated components, which are first order stationary random processes with correlation functions of the form

$K(\tau)=\sigma^2 e^{-\mu|\tau|}$, where σ^2 is the variance of the corresponding error, μ is the damping coefficient of the correlation function, τ is the correlation time; $\boldsymbol{\mu}_{\omega},\boldsymbol{\mu}_n,\boldsymbol{\sigma}_{\omega},\boldsymbol{\sigma}_n$ are matrices of damping coefficients and standard deviations of the corresponding random processes; $\boldsymbol{u}_{f\omega,n}$ are column vectors of unit intensity shaped and centered white noises of gyroscopes and accelerometers; $\Delta\mathbf{k}_{s\omega},\Delta\mathbf{k}_{sn}$ are matrices of scale factors errors and deviations of measurement axes for AU and GU, respectively; $\boldsymbol{1}_R=\boldsymbol{R}(\boldsymbol{R}\cdot\boldsymbol{R})^{-0,5}$ is the vector of geocentric vertical; ω_0 is the natural frequency of an inertial system when an object moves in the vicinity of the Earth surface, usually called Schuler's frequency [25].

6. Mathematical errors model of the displacement sensor

By analogy with the AU and GU, the mathematical errors model of DS can be expressed in the form of systematic and random errors components, as well as scale factor errors:

$$\delta\mathbf{R}_{DSO}=\Delta\mathbf{R}_{DSsys}+\Delta\mathbf{R}_{DSwn}+\Delta\mathbf{R}_{DSstoc}+\Delta\mathbf{k}_{DS}\mathrm{R}_{KO},$$
$$\Delta\dot{\mathbf{R}}_{DSsys}=0,\quad \Delta\dot{\mathbf{R}}_{DSstoc}=-\mu_{DS}\Delta\mathbf{R}_{DSstoc}+\sigma_{DS}\mathbf{u}_{f\mathrm{DS}},\quad \Delta\dot{\mathbf{k}}_{DS}=0 \tag{6.1}$$

where $\Delta\boldsymbol{R}_{DSsys}$ is the vector of DS systematic errors components; $\Delta\boldsymbol{R}_{DSwn}$ is the vector of its random components in the form of white noise; $\Delta\boldsymbol{R}_{DSstoc}$ is the vector of its stochastic autocorrelated components, which is a first order stationary random process with correlation function of the form $K(\tau)$; $\boldsymbol{\mu}_{DS}$, $\boldsymbol{\sigma}_{DS}$ are matrices of damping coefficients and standard deviations of the corresponding random processes; $\boldsymbol{u}_{fDS}$ are column vectors of unit intensity shaped and centered white noises of DS; $\Delta\boldsymbol{k}_{DS}$ is the matrix of scale factors errors and deviations of measurement axes for DS.

As for the case of MEMS IMU1, we consider $\delta\boldsymbol{R}_{ISO}=\delta\boldsymbol{R}_{ISsys}$ – systematic error of the data related to the previously measured $\boldsymbol{R}_{K1}$ and stored in some information source (IS). So, $\delta\dot{\mathbf{R}}_{ISsys}=0$.

7. Kalman filter for open loop correction of VPMS

To achieve acceptable accuracy in measuring vibration parameters we apply OKF estimations and corrections for the orientation and navigation channels (for MEMS IMU1 and MEMS IMU2), as well as for DS. Based on the combined mathematical error model of DS and MEMS IMU2, we can derive the state vector for MEMS IMU2 as follows:

$$\begin{aligned}\delta\boldsymbol{X}=\big(&\theta_\xi,\theta_\eta,\theta_\zeta,\delta U_\xi,\delta U_\eta,\delta U_\zeta,\delta R_\xi,\delta R_\eta,\delta R_\zeta,\Delta\omega_{x\ sys},\Delta\omega_{y\ sys},\Delta\omega_{z\ sys},\Delta n_{x\ sys},\\ &\Delta n_{y\ sys},\Delta n_{z\ sys},\Delta\omega_{x\ stoc},\Delta\omega_{y\ stoc},\Delta\omega_{z\ stoc},\Delta n_{x\ stoc},\Delta n_{y\ stoc},\Delta n_{z\ stoc},\\ &\delta k_x^{s\omega},\delta k_y^{s\omega},\delta k_z^{s\omega},\delta k_x^{sn},\delta k_y^{sn},\delta k_z^{sn},\Theta_{xy}^{\omega},\Theta_{xz}^{\omega},\Theta_{yx}^{\omega},\Theta_{yz}^{\omega},\Theta_{zx}^{\omega},\Theta_{zy}^{\omega},\Theta_{xy}^{n},\Theta_{zx}^{n},\Theta_{zy}^{n},\\ &\delta R_{DS\ x\ sys},\delta R_{DS\ y\ sys},\delta R_{DS\ z\ sys},\delta R_{DS\ x\ stoc},\delta R_{DS\ y\ stoc},\delta R_{DS\ z\ stoc},\\ &\delta k_x^{DS},\delta k_y^{DS},\delta k_z^{DS},\Theta_{xy}^{DS},\Theta_{xz}^{DS},\Theta_{yx}^{DS},\Theta_{yz}^{DS},\Theta_{zx}^{DS},\Theta_{zy}^{DS}\big)^T.\end{aligned} \tag{7.1}$$

where $\delta k^{s\omega,sn,DS}_{x,y,z}$ are the scale factor errors of AU, GU and DS, respectively; $\Theta^{n}_{xy,zx,zy}$ are small deviations angles of the measurement axes of AU; $\Theta^{\omega,DS}_{xy,xz,yx,yz,zx,zy}$ are small deviations angles of the measurement axes of GU and DS, respectively.

By applying the same approach to MEMS IMU1 the state vector will be in the following form:

$$\begin{aligned}\delta \boldsymbol{X} = \big(&\theta_\xi, \theta_\eta, \theta_\zeta, \delta U_\xi, \delta U_\eta, \delta U_\zeta, \delta R_\xi, \delta R_\eta, \delta R_\zeta, \Delta\omega_{x\ sys}, \Delta\omega_{y\ sys}, \Delta\omega_{z\ sys}, \Delta n_{x\ sys},\\ &\Delta n_{y\ sys}, \Delta n_{z\ sys}, \Delta\omega_{x\ stoc}, \Delta\omega_{y\ stoc}, \Delta\omega_{z\ stoc}, \Delta n_{x\ stoc}, \Delta n_{y\ stoc}, \Delta n_{z\ stoc},\\ &\delta k^{s\omega}_{x}, \delta k^{s\omega}_{y}, \delta k^{s\omega}_{z}, \delta k^{sn}_{x}, \delta k^{sn}_{y}, \delta k^{sn}_{z}, \Theta^{\omega}_{xy}, \Theta^{\omega}_{xz}, \Theta^{\omega}_{yx}, \Theta^{\omega}_{yz}, \Theta^{\omega}_{zx}, \Theta^{\omega}_{zy}, \Theta^{n}_{xy}, \Theta^{n}_{zx}, \Theta^{n}_{zy},\\ &\delta R_{IS\ x\ sys}, \delta R_{IS\ y\ sys}, \delta R_{IS\ z\ sys}\big)^{T}.\end{aligned} \tag{7.2}$$

The measurement vector $\mathbf{z}$ for MEMS IMU2 is obtained by comparing the vector $\boldsymbol{R}_{M2}$ (see. Fig.1), calculated according to the measurements of MEMS IMU2, and the same vector calculated according to the readings of DS and NS by vectorial operations using $\boldsymbol{R}_N, \boldsymbol{R}_{K2}, \boldsymbol{R}_{K1}$, taking into account their corrected values. The same applies to MEMS IMU1 considering $\boldsymbol{R}_{M1}, \boldsymbol{R}_N, \boldsymbol{R}_{K1}$, so: $\boldsymbol{z} = \delta\boldsymbol{R}_{M2} - \boldsymbol{A}_{O/ENS}(\delta\boldsymbol{R}_{DSO} + \delta\boldsymbol{R}_{ISO}) - \delta\boldsymbol{R}_{NS}$ for MEMS IMU2, and $\boldsymbol{z} = \delta\boldsymbol{R}_{M1} - \boldsymbol{A}_{O/ENS}\delta\boldsymbol{R}_{ISO} - \delta\boldsymbol{R}_{NS}$ for MEMS IMU1.

Therefore, the system of dynamic and measurement equations could be written as follows:

$$\begin{aligned}&\delta\dot{\mathbf{X}} = \boldsymbol{F}\delta\mathbf{X} + \boldsymbol{G}\boldsymbol{w},\\ &\boldsymbol{z} = \boldsymbol{H}\delta\mathbf{X} + \boldsymbol{v}\end{aligned} \tag{7.3}$$

where $\boldsymbol{F}$ is the dynamic matrix; $\boldsymbol{G}$ is the system noise matrix; $\boldsymbol{w}$ is the system noise vector; $\boldsymbol{v}$ is the measurement noise vector; $\boldsymbol{H}$ is the measurement matrix.

In the discrete form, the OKF algorithm for open loop scheme looks as follows:

$$\begin{aligned}&\boldsymbol{S}_k = \boldsymbol{\Phi}_k \boldsymbol{P}_{k-1} \boldsymbol{\Phi}_k^{T} + \boldsymbol{\Gamma}_k \boldsymbol{Q}_1 \boldsymbol{\Gamma}_k^{T},\\ &\boldsymbol{K}_k = \boldsymbol{S}_k \boldsymbol{H}_k^{T}\left(\boldsymbol{H}_k \boldsymbol{S}_k \boldsymbol{H}_k^{T} + L_1\right)^{-1},\\ &\boldsymbol{P}_k = \left(\boldsymbol{E} - \boldsymbol{K}_k \boldsymbol{H}_k\right)\boldsymbol{S}_k,\\ &\delta\widehat{\boldsymbol{X}}_k = \boldsymbol{\Phi}_k \delta\widehat{\boldsymbol{X}}_{k-1} + \boldsymbol{K}_k\left(\boldsymbol{z}_k - \boldsymbol{H}_k \boldsymbol{\Phi}_k \delta\widehat{\boldsymbol{X}}_{k-1}\right)\end{aligned} \tag{7.4}$$

where $\boldsymbol{\Phi} = \sum_{i=0}^{N} \frac{(\boldsymbol{F}T)^i}{i!}$ – discrete form of $\boldsymbol{F}$; T – calculation step; N – a positive number chosen based on the required discretization accuracy; $\boldsymbol{\Gamma} = \left[\sum_{i=0}^{N} \frac{(\boldsymbol{F}T)^i}{i!(i+1)}\right]\boldsymbol{G}T$ – discrete form of $\boldsymbol{G}$; $\boldsymbol{Q}_1 = \boldsymbol{Q}/T$ – discrete form of system noise dispersion matrix $\boldsymbol{Q}$; $L_1 = L/T$ – discrete form of measurement noise dispersion matrix L; $\boldsymbol{P}$ – state covariance matrix; $\boldsymbol{K}$ – gain matrix of Kalman filter.

Considering that the elements of matrices $\boldsymbol{Q}$, $\boldsymbol{L}$ are not correlated, then these matrices are for MEMS IMU2 diagonals of the form:

$$\boldsymbol{Q} = diag\{\sigma^2_{\Delta\omega_{x\ wn}}\quad \sigma^2_{\Delta\omega_{y\ wn}}\quad \sigma^2_{\Delta\omega_{z\ wn}}\quad \sigma^2_{\Delta n_{x\ wn}}\quad \sigma^2_{\Delta n_{y\ wn}}\quad \sigma^2_{\Delta n_{z\ wn}}\quad 1\ \ 1\ \ 1\ \ 1\ \ 1\ \ 1\ \ 1\ \ 1\ \ 1\},$$

$$\boldsymbol{L} = diag\{\sigma^2_{\Delta R_{x\ DSwn}}\quad \sigma^2_{\Delta R_{y\ DSwn}}\quad \sigma^2_{\Delta R_{z\ DSwn}}\},\qquad (7.5)$$

and for MEMS IMU1 of the form:

$$\boldsymbol{Q} = diag\{\sigma^2_{\Delta\omega_{x\ wn}}\quad \sigma^2_{\Delta\omega_{y\ wn}}\quad \sigma^2_{\Delta\omega_{z\ wn}}\quad \sigma^2_{\Delta n_{x\ wn}}\quad \sigma^2_{\Delta n_{y\ wn}}\quad \sigma^2_{\Delta n_{z\ wn}}\quad 1\ \ 1\ \ 1\ \ 1\ \ 1\ \ 1\};$$

$$\boldsymbol{L} = diag\{\sigma^2_{\Delta R_{x\ Vwn}}\quad \sigma^2_{\Delta R_{y\ VSwn}}\quad \sigma^2_{\Delta R_{z\ Vwn}}\},\qquad (7.6)$$

where $\sigma_{\Delta\omega_{x,y,z\ wn}}$, $\sigma_{\Delta n_{x,y,z\ wn}}$, $\sigma_{\Delta R_{x,y,z\ DSwn}}$ – RMS of random error components of gyroscopes, accelerometers and DS described as white noise; $\sigma_{\Delta R_{x,y,z\ Vwn}}$ – RMS of small artificially generated virtual white noises [21] in the case of MEMS IMU1 (as the IS does not have any white noise).

In this case, it is rational for MEMS IMU2 to choose the initial vector of estimates to be zero, and the initial state covariance matrix to be in the form:

$$\begin{aligned}\boldsymbol{P_0} = diag\{&\sigma^2_{\theta_\xi}, \sigma^2_{\theta_\eta}, \sigma^2_{\theta_\zeta}, \sigma^2_{\delta U_\xi}, \sigma^2_{\delta U_\eta}, \sigma^2_{\delta U_\zeta}, \sigma^2_{\delta R_\xi}, \sigma^2_{\delta R_\eta}, \sigma^2_{\delta R_\zeta},\\ &\sigma^2_{\Delta\omega_{x\ sys}}, \sigma^2_{\Delta\omega_{y\ sys}}, \sigma^2_{\omega_{z\ sys}}, \sigma^2_{\Delta n_{x\ sys}}, \sigma^2_{\Delta n_{y\ sys}}, \sigma^2_{\Delta n_{z\ sys}},\\ &\sigma^2_{\Delta\omega_{x\ stoc}}, \sigma^2_{\Delta\omega_{y\ stoc}}, \sigma^2_{\Delta\omega_{z\ stoc}}, \sigma^2_{\Delta n_{x\ stoc}}, \sigma^2_{\Delta n_{y\ stoc}}, \sigma^2_{\Delta n_{z\ stoc}},\\ &\sigma^2_{\delta k^\omega_x}, \sigma^2_{\delta k^\omega_y}, \sigma^2_{\delta k^\omega_z}, \sigma^2_{\delta k^n_x}, \sigma^2_{\delta k^n_y}, \sigma^2_{\delta k^n_z},\\ &\sigma^2_{\Theta^\omega_{xy}}, \sigma^2_{\Theta^\omega_{xz}}, \sigma^2_{\Theta^\omega_{yx}}, \sigma^2_{\Theta^\omega_{yz}}, \sigma^2_{\Theta^\omega_{zx}}, \sigma^2_{\Theta^\omega_{zy}}, \sigma^2_{\Theta^n_{xy}}, \sigma^2_{\Theta^n_{zx}}, \sigma^2_{\Theta^n_{zy}},\\ &\sigma^2_{\delta R_{x\ DS\ sys}}, \sigma^2_{\delta R_{y\ IS\ sys}}, \sigma^2_{\delta R_{z\ DS\ sys}}, \sigma^2_{\delta R_{x\ дп\ сл}}, \sigma^2_{\delta R_{y\ DS\ stoc}}, \sigma^2_{\delta R_{z\ DS\ stoc}}, \sigma^2_{\delta k^{DS}_x}, \sigma^2_{\delta k^{DS}_y}, \sigma^2_{\delta k^{DS}_z},\\ &\sigma^2_{\Theta^{DS}_{xy}}, \sigma^2_{\Theta^{DS}_{xz}}, \sigma^2_{\Theta^{DS}_{yx}}, \sigma^2_{\Theta^{DS}_{yz}}, \sigma^2_{\Theta^{DS}_{zx}}, \sigma^2_{\Theta^{DS}_{zy}}\},\end{aligned}\qquad (7.7)$$

and for MEMS IMU1 to be in the form:

$$\begin{aligned}\boldsymbol{P_0} = diag\{&\sigma^2_{\theta_\xi}, \sigma^2_{\theta_\eta}, \sigma^2_{\theta_\zeta}, \sigma^2_{\delta U_\xi}, \sigma^2_{\delta U_\eta}, \sigma^2_{\delta U_\zeta}, \sigma^2_{\delta R_\xi}, \sigma^2_{\delta R_\eta}, \sigma^2_{\delta R_\zeta},\\ &\sigma^2_{\Delta\omega_{x\ sys}}, \sigma^2_{\Delta\omega_{y\ sys}}, \sigma^2_{\omega_{z\ sys}}, \sigma^2_{\Delta n_{x\ sys}}, \sigma^2_{\Delta n_{y\ sys}}, \sigma^2_{\Delta n_{z\ sys}},\\ &\sigma^2_{\Delta\omega_{x\ stoc}}, \sigma^2_{\Delta\omega_{y\ stoc}}, \sigma^2_{\Delta\omega_{z\ stoc}}, \sigma^2_{\Delta n_{x\ stoc}}, \sigma^2_{\Delta n_{y\ stoc}}, \sigma^2_{\Delta n_{z\ stoc}},\\ &\sigma^2_{\delta k^\omega_x}, \sigma^2_{\delta k^\omega_y}, \sigma^2_{\delta k^\omega_z}, \sigma^2_{\delta k^n_x}, \sigma^2_{\delta k^n_y}, \sigma^2_{\delta k^n_z},\\ &\sigma^2_{\Theta^\omega_{xy}}, \sigma^2_{\Theta^\omega_{xz}}, \sigma^2_{\Theta^\omega_{yx}}, \sigma^2_{\Theta^\omega_{yz}}, \sigma^2_{\Theta^\omega_{zx}}, \sigma^2_{\Theta^\omega_{zy}}, \sigma^2_{\Theta^n_{xy}}, \sigma^2_{\Theta^n_{zx}}, \sigma^2_{\Theta^n_{zy}},\\ &\sigma^2_{\delta R_{x\ IS\ sys}}, \sigma^2_{\delta R_{y\ IS\ sys}}, \sigma^2_{\delta R_{z\ IS\ sys}}\}\end{aligned}\qquad (7.8)$$

where $\sigma_{\theta_{\xi,\eta,\zeta}}$, $\sigma_{\delta U_{\xi,\eta,\zeta}}$, $\sigma_{\delta R_{\xi,\eta,\zeta}}$ – RMS of initial alignment errors by orientation parameters, relative velocity and positioning, respectively; $\sigma_{\Delta\omega x,y,z\ sys}$, $\sigma_{\Delta nx,y,z\ sys}$, $\sigma_{\delta R_{x,y,z\ DS\ sys}}$, $\sigma_{\delta R_{x,y,z\ IS\ sys}}$ – RMS of systematic errors realization for the gyroscopes, accelerometers, DS and IS, respectively; $\sigma_{\Delta\omega x,y,z\ stoc}$, $\sigma_{\Delta nx,y,z\ stoc}$ – RMS of gyroscopes and accelerometers random errors, respectively; $\sigma_{\delta k^{\omega}_{x,y,z}}$, $\sigma_{\delta k^{n}_{x,y,z}}$, $\sigma_{\delta k^{DS}_{x,y,z}}$ – RMS of gyroscopes, accelerometers and DS scaling factors errors realization, respectively; $\sigma_{\Theta^{\omega}_{xy,xz,yx,yz,zx,zy}}$, $\sigma_{\Theta^{n}_{xy,zx,zy}}$, $\sigma_{\Theta^{DS}_{xy,xz,yx,yz,zx,zy}}$ – RMS of gyroscopes, accelerometers and DS measurement axes deviations errors realization, respectively.

For the open loop correction [20], the estimates of main system errors are formed using OKF estimates for the most general case of MEMS IMU2 as follows:

$$\begin{aligned}
&\hat{\boldsymbol{U}} = \boldsymbol{U}_{\mathrm{C}} - \delta\hat{\boldsymbol{U}}, \quad \hat{\boldsymbol{R}} = \boldsymbol{R}_{\mathrm{C}} - \delta\hat{\boldsymbol{R}}, \quad \hat{\boldsymbol{A}}_{\mathrm{O/E}} = (\boldsymbol{E} + \boldsymbol{K}_{\hat{\theta}})\boldsymbol{A}_{\mathrm{O/EC}},\\
&\hat{\boldsymbol{\omega}}_{\mathrm{O}} = \boldsymbol{\omega}_{\mathrm{O_C}} - (\Delta\hat{\boldsymbol{\omega}}_{\mathrm{sys}} + \Delta\hat{\boldsymbol{\omega}}_{\mathrm{stoc}} + \Delta\hat{\boldsymbol{k}}_{\mathrm{s\omega}}\boldsymbol{\omega}_{\mathrm{OC}}),\\
&\hat{\boldsymbol{n}}_{\mathrm{O}} = \boldsymbol{n}_{\mathrm{OC}} - (\Delta\hat{\boldsymbol{n}}_{\mathrm{sys}} + \Delta\hat{\boldsymbol{n}}_{\mathrm{stoc}} + \Delta\hat{\boldsymbol{k}}_{\mathrm{sn}}\boldsymbol{n}_{\mathrm{OC}}),\\
&\hat{\mathbf{R}}_{\mathrm{KO}} = \mathbf{R}_{\mathrm{KOC}} - (\Delta\hat{\mathbf{R}}_{\mathrm{DSsys}} + \Delta\hat{\mathbf{R}}_{\mathrm{DSstoc}} + \Delta\hat{\mathbf{k}}_{\mathrm{DS}}\boldsymbol{R}_{\mathrm{KO}}),\\
&\dot{\hat{\boldsymbol{U}}} = \dot{\boldsymbol{U}}_{\mathrm{C}} + 2\boldsymbol{u}\times\delta\hat{\boldsymbol{U}} - \hat{\boldsymbol{A}}_{\mathrm{O/E}}(\Delta\hat{\boldsymbol{n}}_{\mathrm{sys}} + \Delta\hat{\boldsymbol{n}}_{\mathrm{stoc}} + \Delta\hat{\boldsymbol{k}}_{\mathrm{sn}}\boldsymbol{n}_{\mathrm{OC}}) +\\
&+\hat{\boldsymbol{\theta}}\times(\hat{\boldsymbol{A}}_{\mathrm{O/E}}\hat{\boldsymbol{n}}_{\mathrm{O}}) + \omega_0^2\left(\delta\hat{\boldsymbol{R}} - 3\left(\delta\hat{\boldsymbol{R}}\cdot\boldsymbol{1}_{\hat{\mathrm{R}}}\right)\boldsymbol{1}_{\hat{\mathrm{R}}}\right)
\end{aligned} \tag{7.9}$$

where $\hat{\mathrm{X}}$ is the estimate of X, obtained by OKF; the index $_C$ indicates that the corresponding vector is calculated; $\boldsymbol{K}_{\hat{\theta}}$ is the skew-symmetric matrix composed by the elements of $\hat{\boldsymbol{\theta}}$; $\mathbf{E}$ – unit matrix.

For MEMS IMU1 we need to eliminate $\Delta\hat{\mathbf{R}}_{\mathrm{DSstoc}}$, $\Delta\hat{\mathbf{k}}_{\mathrm{DS}}$, and replace $\Delta\hat{\mathbf{R}}_{\mathrm{DSsys}}$ by $\delta\hat{\boldsymbol{R}}_{ISsys}$.

8. Closed-loop optimal correction algorithm of VPMS

As we have already mentioned, the open loop scheme gives an acceptable result only for a limited period of time [21]. To overcome this problem it is advisable to use closed-loop optimal correction, where a feedback correction signal is formulated as a product of the measurement vector by Kalman filter optimal gains matrix ($\boldsymbol{K}$). In this case, the operation algorithm in the case of MEMS IMU2 can be formulated in the form of (8.1), where $\mathbf{z} = \boldsymbol{R} - (\boldsymbol{R}_{NC} + \boldsymbol{A}_{O/ENC}(\boldsymbol{R}_{K2OC} + \boldsymbol{R}_{K1O\varepsilon} - \Delta\hat{\boldsymbol{R}}_{DSsys} - \Delta\hat{\boldsymbol{R}}_{DSstoc} - \Delta\hat{\mathbf{k}}_{DS}\boldsymbol{R}_{K2OC}))$ is the measurement vector for the most general case MEMS IMU2. Moreover, the symbol $\boldsymbol{R}$ is used in (8.1) in order to keep the generality of (4.1) and (5.1). On the other hand, when it is difficult or impossible to implement the "closure" using correction signals for some parameters in the system under consideration, due to many physical or technical reasons, it is possible to realize it using the estimates of these parameters. In such case, the correction scheme is sometimes called mixed closed – open correction:

$$\dot{\boldsymbol{\Lambda}} = 0{,}5\boldsymbol{M}_{(\boldsymbol{\omega}_O - \Delta\hat{\boldsymbol{\omega}}_{sys} - \Delta\hat{\boldsymbol{\omega}}_{stoc} - \Delta\hat{\mathbf{k}}_{s\omega}\boldsymbol{\omega}_O + \boldsymbol{A}^{\mathrm{T}}_{O/E}\boldsymbol{K}^{<0-2>}\mathbf{z})}\boldsymbol{\Lambda}, \tag{8.1}$$

$$A_{O/E} = \begin{pmatrix} \cos(u_0 t) & \sin(u_0 t) & 0 \\ -\sin(u_0 t) & \cos(u_0 t) & 0 \\ 0 & 0 & 1 \end{pmatrix} \left[\left(2\lambda_0^2 - 1\right) \boldsymbol{E} + 2\left[\boldsymbol{\lambda\lambda}^{\mathrm{T}} \right] - 2\lambda_0 \boldsymbol{K}_{\lambda} \right],$$

$$\dot{\boldsymbol{U}} = -2\boldsymbol{u} \times \boldsymbol{U} + \boldsymbol{A}_{O/E}\left(\boldsymbol{n}_O - \widehat{\Delta \boldsymbol{n}}_{sys} - \widehat{\Delta \boldsymbol{n}}_{stoc} - \widehat{\Delta \mathbf{k}}_{sn}\boldsymbol{n}_O\right) + \boldsymbol{g}_N - \boldsymbol{K}^{<3-5>}\mathbf{z},$$

$$\dot{\boldsymbol{R}} = \boldsymbol{U} - \boldsymbol{K}^{<6-8>}\mathbf{z}, \quad \widehat{\Delta \dot{\boldsymbol{\omega}}}_{sys} = \boldsymbol{K}^{<9-11>}\mathbf{z}, \quad \widehat{\Delta \dot{\boldsymbol{n}}}_{sys} = \boldsymbol{K}^{<12-14>}\mathbf{z},$$

$$\widehat{\Delta \dot{\boldsymbol{\omega}}}_{stoc} = -\boldsymbol{\mu}_{\omega}\widehat{\Delta \boldsymbol{\omega}}_{stoc} + \boldsymbol{K}^{<15-17>}\mathbf{z}, \quad \widehat{\Delta \dot{\mathbf{n}}}_{stoc} = -\boldsymbol{\mu}_n \widehat{\Delta \mathbf{n}}_{stoc} + \boldsymbol{K}^{<18-20>}\mathbf{z},$$

$$\widehat{\delta \dot{\boldsymbol{k}}}_{s\omega} = \boldsymbol{K}^{<21-23>}\mathbf{z}, \quad \widehat{\delta \dot{\boldsymbol{k}}}_{sn} = \boldsymbol{K}^{<24-26>}\mathbf{z}, \tag{cont.Eq.8.1}$$

$$\dot{\widehat{\Theta}}^{\omega} = \boldsymbol{K}^{<27-32>}\mathbf{z}, \quad \dot{\widehat{\Theta}}^{n} = \boldsymbol{K}^{<33-35>}\mathbf{z},$$

$$\widehat{\Delta \dot{\mathbf{R}}}_{DSsys} = \boldsymbol{K}^{<36-38>}\boldsymbol{z}, \quad \widehat{\Delta \dot{\mathbf{R}}}_{DSstoc} = -\boldsymbol{\mu}_{DS}\widehat{\Delta \mathbf{R}}_{DSstoc} + \boldsymbol{K}^{<39-41>}\boldsymbol{z},$$

$$\widehat{\delta \dot{\mathbf{k}}}_{DS} = \boldsymbol{K}^{<42-44>}\boldsymbol{z}, \quad \dot{\widehat{\Theta}}^{DS} = \boldsymbol{K}^{<45-50>}\mathbf{z},$$

$$\mathbf{z} = \boldsymbol{R} - (\boldsymbol{R}_{NC} + \boldsymbol{A}_{O/ENC}(\boldsymbol{R}_{K2OC} + \boldsymbol{R}_{K1O\varepsilon} - \widehat{\Delta \boldsymbol{R}}_{DSsys} - \widehat{\Delta \boldsymbol{R}}_{DSstoc} - \widehat{\Delta \boldsymbol{k}}_{DS}\boldsymbol{R}_{K2OC}))$$

where $\boldsymbol{R}_{NC}, \boldsymbol{A}_{O/ENC}$ – calculated by the high-precision onboard NS; index $^{<i-j>}$ shows that the rows from the i^{th} to the j^{th} in the matrix $\boldsymbol{K}$ are used; $\widehat{\mathrm{X}}$ denotes an estimate of the error of the corresponding calculated quantity X; $\boldsymbol{R}_{K1Oe} = (\boldsymbol{R}_{K1OC} - \widehat{\delta \boldsymbol{R}}_{ISsys})$ – calculated $\boldsymbol{R}_{K1}$ after the estimate correction using OKF corresponded to MEMS IMU1. For the case of MEMS IMU1, the operation algorithm is constructed by analogy with (8.1), but $\widehat{\delta \dot{\mathbf{R}}}_{ISsys}$ is used instead of $\widehat{\Delta \dot{\mathbf{R}}}_{DSsys}$, and the equations of estimates after it are eliminated, and the equation for the formation of the measurement vector in this case has the form of $\mathbf{z} = \boldsymbol{R} - (\boldsymbol{R}_{NC} + \boldsymbol{A}_{O/ENC}(\boldsymbol{R}_{K1OC} - \widehat{\delta \boldsymbol{R}}_{ISsys}))$. By using $\widehat{\boldsymbol{A}}_{\mathrm{O/E}M1}$ (7.9) which is the estimated value of $\boldsymbol{A}_{O/E}$ for MEMS IMU1, as well as the corrected $\boldsymbol{R}$, $\boldsymbol{U}$, $\dot{\boldsymbol{U}}$ for MEMS IMU1 and MEMS IMU2, it is easy to calculate the required vibration parameters (vibration displacement, vibration velocity and vibration acceleration) in ACS using the following equations:

$$\widehat{\boldsymbol{R}}_{\mathrm{K2O}} = \widehat{\boldsymbol{A}}^{\mathrm{T}}_{\mathrm{O/E}M1}(\boldsymbol{R}_{\mathrm{M2C}} - \boldsymbol{R}_{\mathrm{M1C}}),$$

$$\widehat{\boldsymbol{U}}_{\mathrm{K2O}} = \widehat{\boldsymbol{A}}^{\mathrm{T}}_{\mathrm{O/E}M1}(\boldsymbol{U}_{\mathrm{M2C}} - \boldsymbol{U}_{\mathrm{M1C}}), \tag{8.2}$$

$$\widehat{\dot{\boldsymbol{U}}}_{\mathrm{K2O}} = \widehat{\boldsymbol{A}}^{\mathrm{T}}_{\mathrm{O/E}M1}(\dot{\boldsymbol{U}}_{\mathrm{M2C}} - \dot{\boldsymbol{U}}_{\mathrm{M1C}}).$$

8. Simulation results

The simulation of the proposed VPMS model was performed in order to make an assessment of the expected accuracy characteristics of the system. The case study considered an aircraft parked while the engines and onboard equipment are turned on, which in turn causes the generation of random and harmonic linear and angular vibrations of the aircraft wing, whose amplitudes are in the orders of $0.065m$ and $3.5°$, respectively.

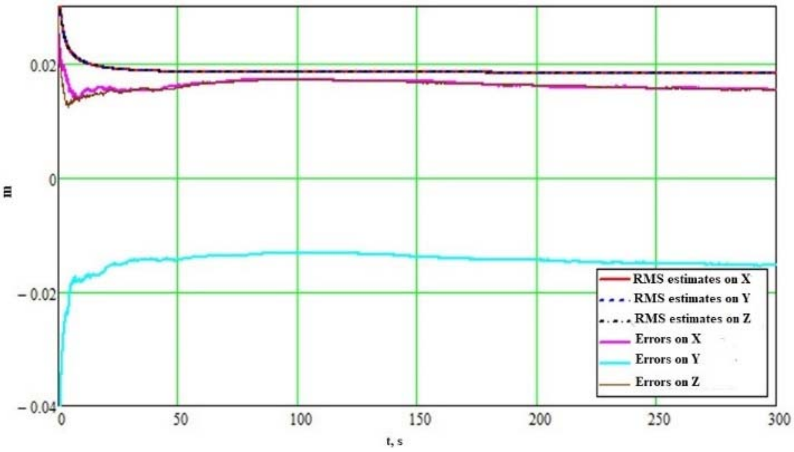

Fig.2. The residual errors when determining vibration displacement projections, and their RMS estimates in ACS.

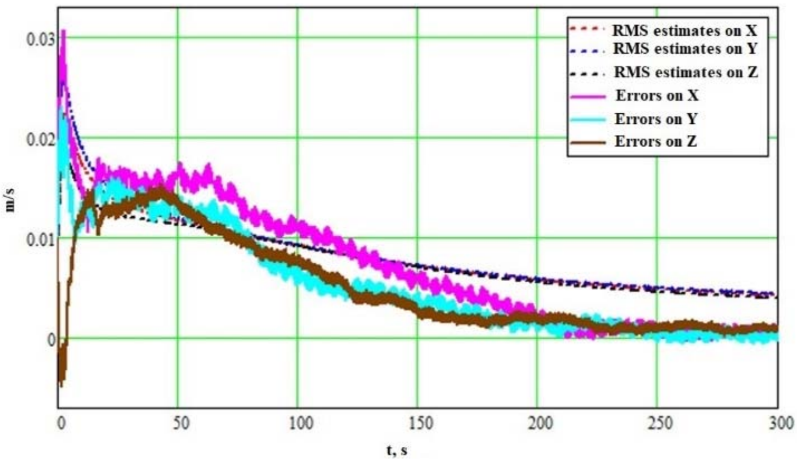

Fig.3. The residual errors when determining vibration velocity projections, and their RMS estimates in ACS.

The systematic errors of AU and GU and their standard deviations of the random components are selected at the order of $0.3°/h$, $0.001\,m/s^2$, respectively, whereas the systematic errors of the onboard NS by coordinates and velocity were $20\,m$ and $0.1\,m/s$. The DS errors, the systematic components and the RMS of random components, are $0.02\,m$. The initial alignment errors regarding the orientation and navigation parameters of both MEMS IMU1, 2 are $10^{-2}\,rad$, $10\,m$, $0.05\,m/s$. The distance from NS to MEMS IMU1 is $1.1\,m$, and to MEMS IMU2 is $9.6\,m$. Figures 2 to 5 show the simulation results, from which it can be seen that for the proposed VPMS, the results of estimating the expected accuracy turned out to be quite acceptable, since over a time interval of $200\text{-}250\,s$, the residual errors of vibration displacement and vibration velocity are settled down at levels of the order of $0.016\text{-}0.018\,m$ and $0.002\text{-}0.005\,m/s$, respectively.

In addition, it was possible to estimate the systematic errors components of vertical accelerometer and horizontal gyroscopes with a high degree of accuracy at the level of $0.0003-0.0004 m/s^2$ and $0.06-0.08°/h$, respectively. At the same time, in this case, the errors of horizontal accelerometers and vertical gyroscope are practically not estimated.

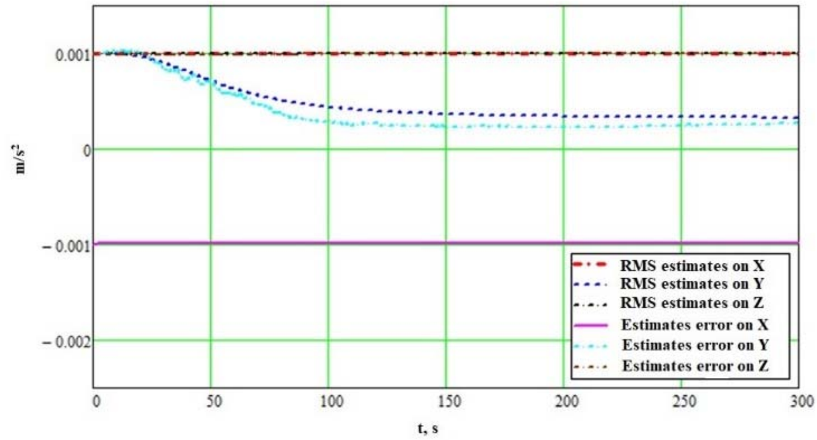

Fig.4. The estimates of systematic error components of accelerometers, and their RMS estimates in ACS.

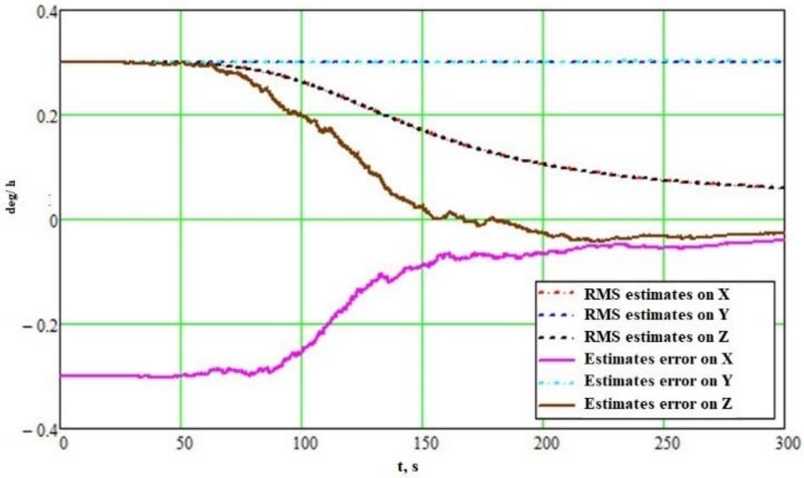

Fig.5. The estimates of systematic error components of gyroscopes, and their RMS estimates in ACS.

9. Discussion

The above system simulation results show that by using the proposed technique of "closing" the scheme of OKF incorporation wherever available, it is possible to provide continuous correction of VPMS orientation and navigation channels in such a way that their final errors remain at small values for a long time, i.e. following the used basic linear error mathematical models. Consequently, this will effectively overcome the main drawback of MEMS IMU, namely its significant inherent errors and high instability of its characteristics, which usually lead to rapid growth of orientation and navigation channels errors, even for a short period of time, and the errors can then strongly deviate from the corresponding error models. That is why in this case the traditional open-loop correction scheme of OKF incorporation may be ineffective, especially for solving vibration measurement problems. The simulation results also show a poor estimation of horizontal accelerometers and vertical gyroscope errors, which could be explained by the fact that the aircraft is in a stationary mode relative to the Earth, when the movements of MEMS IMU2 are limited by the vibrations of the wing tip only. It is assumed that, for example, in a more general case, with dynamic movement of the aircraft, the corresponding estimates could get significantly better.

10. Conclusion

It is shown in this work that, based on the use of MEMS IMU, optimal Kalman estimation algorithms, and a closed-loop optimal correction, a promising VPMS of aircraft wing can be constructed. The proposed system will have many advantages over the existing analogue systems, including among other things simplicity, acceptable degree of accuracy, low cost, low weight. Moreover, the system structure allows expanding its functionality relatively simply by increasing the required number of measurement points. In addition, it is assumed that the system can be used not only in ground conditions, but also in the in-flight operation mode. The initial results obtained from simulation confirm the operability and acceptable accuracy of the system in the case of a stationary operation mode of the aircraft. At the subsequent stages of research, it is intended to simulate the operation of the proposed VPMS for in-flight and maneuvering flight cases under conditions of significant overloads and high vibrations. Finally, it is expected that the proposed method for measuring the vibration parameters of aircraft structural elements, particularly in difficult flight conditions, would be in demand and useful, for example, for monitoring the state of aircraft structural elements, predicting the appearance and development of their defects throughout their entire operation cycle.

Acknowledgments

This work was supported by Russian Foundation for Basic Research (RFBR) (research project no. 19-08-00279a), supervised by the Government of Russian Federation.

Nomenclature

$\boldsymbol{A}_{O/E}$	– orientation matrix of ECS relative to ACS
ACS	– right coordinate system associated with MEMS IMU
AU	– accelerometers unit
DS	– displacement sensor
$\boldsymbol{E}$	– unit matrix
ECS	– right Earth equatorial (Greenwich) coordinate system
$\boldsymbol{g}_N$	– vector of normal gravitational acceleration
GU	– gyroscopes unit
$\boldsymbol{K}$	– Kalman filter optimal gains matrix
K(τ)	– correlation function
$\boldsymbol{K}_\lambda$	– skew-symmetric matrix composed of $\boldsymbol{\lambda} = [\lambda_1, \lambda_2, \lambda_3]^T$ elements
$\boldsymbol{M}_{\omega_O}$	– skew-symmetric (quaternionic) 4x4 matrix composed of $\boldsymbol{\omega}_O$ projections
MEMS IMU	– microelectromechanical inertial measurement unit
NS	– navigation system
$\boldsymbol{n}_O$	– apparent acceleration vector
$\boldsymbol{R}$	– geocentric radius vector
RMS	– root mean square
$\boldsymbol{u}$	– vector of the angular velocity of Earth's own rotation

$\boldsymbol{U}$ – velocity

$\dot{\boldsymbol{U}}$ – acceleration

VPMS – vibration parameters measurement system

$\mathbf{z}$ – measurement vector

$\boldsymbol{\theta}$ – vector of small rotations characterizing the inclination of ECS calculated position relative to its true position

$\Delta \boldsymbol{k}_{DS}$ – matrix of scale factors errors and deviations of measurement axes for DS

$\Delta \mathbf{k}_{sn}$ – matrix of scale factors errors and deviations of measurement axes for AU

$\Delta \mathbf{k}_{s\omega}$ – matrix of scale factors errors and deviations of measurement axes for GU

$\Delta \boldsymbol{n}_{wn}$ – vector of random components of AU errors in the form of white noise

$\Delta \boldsymbol{n}_{stoc}$ – vector of random (stochastic) autocorrelated components of AU errors

$\Delta \boldsymbol{n}_{sys}$ – vector of systematic errors components of AU

$\Delta \boldsymbol{R}_{DSstoc}$ – vector of random (stochastic) autocorrelated components of DS

$\Delta \boldsymbol{R}_{DSsys}$ – vector of DS systematic errors components

$\Delta \boldsymbol{R}_{DSwn}$ – vector of random errors component of DS errors in the form of white noise

$\Delta \boldsymbol{\omega}_{stoc}$ – vector of random (stochastic) autocorrelated components of GU errors

$\Delta \boldsymbol{\omega}_{sys}$ – vector of systematic errors components of GU

$\Delta \boldsymbol{\omega}_{wn}$ – vector of random components of GU errors in the form of white noise

$\boldsymbol{\Lambda} = [\lambda_0, \lambda_1, \lambda_2, \lambda_3]^T$ – vector of Rodrigues-Hamilton parameters

$\Delta, \ \delta$ – errors

σ^2 – variance of the corresponding error

μ – damping coefficient of the correlation function

τ – correlation time

$\boldsymbol{\omega}_O$ – absolute angular velocity vector

ω_0 – Schuler's frequency

$\boldsymbol{1}_R$ – vector of geocentric vertical

References

[1] Krysinski T. and Malburet F. (2010): *Mechanical Vibrations: Active and Passive Control*.– John Wiley & Sons.

[2] Burns V.A., Lysenko E.A., Marinin D.A., Dolgopolov A.V. and Zhukov E.P. (2015): *Identification .of aircraft defects by vibration parameters during operation*.– Academy of Sciences of the Higher School of the Russian Federation Reports, vol.2, pp.24-42.

[3] Komarov V.A. and Lapteva M.Yu. (2011): *Predicting wing deformations*.– All-Russian Scientific-Technical Journal "Polyot" ("Flight"), vol.3, pp.7-12.

[4] Parputs A.A., Pankeev E.S. and Musonov V.M. (2015): *vibration tests of designs aircraft*.– Actual problems of aviation and astronautics, vol.1, No.11, 714-715.

[5] Feigenbaum Yu.M., Butushin S.V., Bozhevalov D.G. and Sokolov Yu.S. (2015): *Composite materials and the history of their implementation in aircraft structures*.– Scientific Bulletin of GosNII GA, vol.7, pp.24-37.

[6] Katunin A., Dragan K. and Dziendzikowski M. (2015): *Damage identification in aircraft composite structures: A case study using various non-destructive testing techniques*.– Composite structures, vol.127, pp.1-9.

[7] Pang Z.Y., Cesnik C.E., Atkins E.M. (2014): *In-flight wing deformation measurement system for small unmanned aerial vehicles*.– In 55th AIAA/ASMe/ASCE/AHS/SC Structures, Structural Dynamics and Materials Conference, p.0330.

[8] Alvarez-Montoya J., Carvajal-Castrillón A. and Sierra-Pérez J. (2020): *In-flight and wireless damage detection in a UAV composite wing using fiber optic sensors and strain field pattern recognition*.– Mechanical Systems and Signal Processing, vol.136, p.106526.

[9] Varanis M., Silva A., Mereles A. and Pederiva R. (2018): *MEMS accelerometers for mechanical vibrations analysis: A comprehensive review with applications*.– Journal of the Brazilian Society of Mechanical Sciences and Engineering, vol.40, No.11, pp.1-18.

[10] Govers Y., Sinske J. and Petzsche T. (2020): *Latest design trends in modal accelerometers for aircraft ground vibration testing*.– In Sensors and Instrumentation, Aircraft/Aerospace, Energy Harvesting & Dynamic Environments Testing, Springer, Cham, vol.7, pp.97-106.

[11] Looney M. (2012): *Analyzing Frequency Response of Inertial MEMS in Stabilization Systems*.– Analog Dialogue, p.46.

[12] Yates Jr. E.C. (1985): *AGARD standard aeroelastic configurations for dynamic response I-wing 445.6*.– 61st Meeting of the structures and materials panel, Germany.

[13] Shokrieh M.M. and Behrooz F.T. (2001): *Wing instability of a full composite aircraft*.– Composite structures, vol.54, No.2-3, pp.335-40.

[14] Aggarwal P. (2010): *MEMS-based integrated navigation*.– Artech House.

[15] Hemerly E.M. (2017): *MEMS IMU stochastic error modelling*.– Systems Science and Control Engineering, vol.5, No.1, pp.1-8.

[16] Syed Z.F., Aggarwal P., Goodall C., Niu X. and El-Sheimy N. (2007) *A new multi-position calibration method for MEMS inertial navigation systems*.– Measurement Science and Technology, vol.18, No.7, Article Number.1897.

[17] Kaswekar P. and Wagner J.F. (2015): *Sensor fusion based vibration estimation using inertial sensors for a complex lightweight structure*.– In 2015 DGON Inertial Sensors and Systems Symposium (ISS), IEEE, pp.1-20.

[18] Chui C.K. and Chen G. (2017): *Kalman filtering*.– Berlin, Germany: Springer International Publishing.

[19] Alvarez-Montoya J., Carvajal-Castrillón A. and Sierra-Pérez J. (2020): *In-flight and wireless damage detection in a UAV composite wing using fiber optic sensors and strain field pattern recognition*.– Mechanical Systems and Signal Processing, vol.136, Article Number.106526.

[20] Afonin A.A., Sulakov A.S. and Maamo M.S. (2021) *Application of optimal Kalman filter to improve the accuracy of aircraft wing vibration parameters measurement system*. Journal of Physics: Conference Series, vol.2096, No.1, p. 012182. IOP Publishing.

[21] Rivkin S.S., Ivanovsky R.I. and Kostrov A.V. (1976): *Statistical Optimization of Navigation Systems*.– Shipbuilding in Leningrad, p.280.

[22] Afonin A.A. and Sulakov A.S. (2011): *About the correction of the parameters of orientation, navigation and gravimetry in a closed circuit for switching on the Kalman filter of the navigation complex*.– Aerospace Instrument-Making, vol.8, pp.17-24.

[23] Tyvin A.V., Afonin A.A. and Chernomorsky A.I. (2005): *About one concept of vector gravimetric .measurements*.– Journal Aerospace Instrumentation, vol.3, pp.24-29.

[24] Alyoshin B.S., Afonin A.A. and Veremeenko K.K. (2006): *Orientation and Navigation of Movable Objects: Modern Information Technologies*.– Moscow, Fizmatlit, p.421.

[25] Andreev V.D. (1966): *Inertial Navigation Theory: Autonomous Systems*.– Publishing House "Science", Head. ed. Physics and Mathematics Literature.

Received: November 11, 2021
Revised: March 1, 2022